Advanced ultra-light multifunctional metallic-glass wave springs

N.T. Panagiotopoulos, K. Georgarakis, A.M. Jorge Jr, M. Aljerf, W.J. Botta, A.L. Greer, A.R. Yavari

Version of Record: https://www.sciencedirect.com/science/article/pii/S026412752030304X
Manuscript_3bf400f90f6211f7ee4eff0e8a439149

Advanced ultra-light multifunctional metallic-glass wave springs

N.T. Panagiotopoulos[1,2,*], K. Georgarakis[1,3,*], A.M. Jorge Jr[1,4], M. Aljerf[1], W.J. Botta[4], A.L. Greer[2], A.R. Yavari[1,†]

[1] Univ. Grenoble Alpes, CNRS, Grenoble INP, SIMaP, F-38000 Grenoble, France
[2] University of Cambridge, Department of Materials Science & Metallurgy, Cambridge CB3 0FS, UK
[3] School of Aerospace, Transport and Manufacturing, Cranfield University, MK43 0AL, UK
[4] Federal University of São Carlos, DEMa, São Carlos, SP, 13565-905, Brazil
[†]deceased

[*] Corresponding author:
np488@cam.ac.uk (N.T. Panagiotopoulos)

Abstract

We show that, using thermo-elastic processing, metallic-glass foils can be shaped, without being embrittled, into linear and annular wave springs. These springs exhibit an undulatory behaviour, unique to metallic-glass foils, in which under compression the number of arcs in the spring increases, increasing the load-bearing capacity and the spring constant. We evaluate the performance limits of the metallic-glass wave springs, and consider how the undulatory behaviour can be exploited. The metallic-glass springs can operate over the same load-ranges as commercially available crystalline wave springs, but have material volumes (and therefore weights) that are one to two orders of magnitude less. Their energy storage per unit material volume is as high as 2600 kJ m^{-3}. We suggest that the undulatory behaviour is important in rendering the springs fail-safe in case of overload. We discuss the range of applicability of thermo-elastic processing, the likely working limit of metallic-glass wave springs, and the potential for application of metallic-glass springs in MEMS devices.

Keywords: metallic glasses, wave springs, shaping, elastic behaviour, embrittlement, energy storage.

1. Introduction

Metallic glasses (MGs) find applications as advanced materials because of their exceptional combination of properties [1–5]. Due to their amorphous structure, MGs show high elastic limit [6,7] and strength [6], and good soft-magnetic [8,9] and anticorrosion [10] properties. Various methods have been used for thermoplastic forming of MGs while maintaining their amorphous structure and exceptional properties [5,11–14]. Because the MGs are metastable and liable to crystallize, these forming processes require rapid heating and short times. Even without any crystallization, however, heating of MGs allows them to undergo structural relaxation to denser glassy states, and this, especially for Fe-based MGs, can lead to severe embrittlement [15].

However, Aljerf et al. [15] showed that shaping without embrittlement can be achieved by *thermo-elastic processing* (TEP), in which a sample, elastically deformed to a particular shape, is carefully annealed to relax the stresses in the sample, permitting it to fully or partially adopt the imposed shape. In this way, thin MG foils can be uniformly shaped into complex forms, as has been demonstrated for a variety of alloys, including binary ($Co_{80}B_{20}$, $Fe_{83}B_{17}$, and $Pd_{82}Si_{18}$), ternary ($Cu_{60}Zr_{30}Al_{10}$ and $Fe_{81.5}B_{14.5}Si_4$) and quaternary ($Fe_{40}Ni_{40}Si_6B_{14}$ and $Zr_{70}Ni_{16}Cu_6A_{18}$) compositions (here, in at.%) [15,16].

MGs are particularly attractive for the development of superior springs, as demonstrated, for example, for coil springs [17,18]. Recently, we reported a unique undulatory behaviour of MG foils rendered possible by their high elastic limit [19,20]. An Fe-based MG ribbon, elastically bent into an arc-shape is subjected to a normal load at the crest of the arc. The ribbon develops a wave-like pattern, and as the load is increased, additional waves appear, shortening the wavelength. As long as the deformation remains in the elastic region (i.e. the number of multiplied arcs remains below a critical limit), the undulatory behaviour is reversible, functioning as a flat spring with multiple spring constants [19]. This reversible undulatory behaviour of MG foils showed resistance to fatigue of the order of thousands of cycles, while crystalline ribbons show no reversibility at all as they undergo plastic deformation during the first loading [19,20]. Moreover, a novel electromechanical switch has been proposed [19].

Thin MG foils with the dimensions of interest in the present study are produced industrially. They have a thickness of some tens of micrometres, and are made by planar-flow casting; glass formation is achieved because of the ultra-high cooling rates in this process [21,22].

The range of conventional springs includes *wave springs*, in which a linear (strip) or annular (washer) piece of flat material is formed into a wavy shape. Such linear and washer wave springs are particularly useful when space is limited, and they also use less material than coil springs [23].

In this communication, we report on the design, manufacture and performance of novel multifunctional MG wave springs. Using the principles suggested in [15], Cr-bearing Fe-based MG foils are shaped by TEP without thermal embrittlement to form linear and annular wave springs. The pre-shaped MG foils can function as free-standing flat springs over a wide range of load. Furthermore, the geometrical characteristics of these linear and annular pre-shaped wavy patterns are designed to further exploit the undulatory behaviour of MG foils. We show that the pre-shaped wavy MG foils do transform their geometry after a load threshold, avoiding plastic deformation while increasing their load capacity. In this way, much more of the elastic-energy storage capacity of the MG can be exploited. After load release, the wave patterns return to their initial pre-shaped form. This synergetic mechanism of pre-formed and newly developed waves is proposed for the production of advanced and durable MG flat springs with tunable spring stiffness.

2. Experimental details

Commercial Fe-based MG foils [Metglas 2605S3A, Fe: 85–95%, B: 1–5%, Cr: 1–5 %, Si: 1–5% (wt.%)] of 20 μm thickness and 25 mm width, produced by planar-flow casting, were obtained from Metglas Inc. (Conway, SC). Two free-standing types of wave springs (linear and annular) were fabricated by TEP. The linear waveform was obtained by weaving a length of MG foil past alternating sides of nine parallel metallic rods. The axis-to-axis spacing of the rods was 2.8 mm, allowing the fabrication of a waveform 28 mm long and covering five wavelengths of 5.6 mm. Rings of 20 mm outer and 10 mm inner diameter for the annular waveform were cut from a flat MG foil by electroerosion (0.5 A applied via a 180 μm diameter wire). A cylindrical two-piece stainless-steel die was designed and fabricated in which the annular foils were placed to impose the waveform.

In each case (for linear and annular waveforms), the shaping assemblies (MG foil and die) were annealed in a preheated furnace under inert argon atmosphere, then rapidly quenched in water. The shaped foils were rinsed with alcohol and finally dried under air flow. Annealing temperatures up to 360°C were used, well below the crystallization temperature

(T_x = 516°C, determined by differential scanning calorimetry using a NETZSCH DSC 404 instrument with a heating rate of 10 K min^{-1}) of the MG; the temperature was recorded at the exact position of the sample using a thermocouple. For the shaping of the linear waveforms, the low thermal mass of the forming assembly allowed relatively high heating rates of 80–100 K min^{-1} to be achieved. In contrast, the thermal mass of the annular-waveform die limited the heating rate in that case to 5–15 K min^{-1}.

The radius of curvature was measured after each annealing process using image analysis tools (ImageJ software) [24]. The extent of the shaping can be characterized by the *shaping factor*, R_0/R, where R_0 is the radius of curvature of the shaping die surface and R is the radius of curvature of the formed foil. Without heating, the shaping factor is zero, since on release from the die, the MG foil elastically recovers to its initial state. The shaping factor can reach 100% for thermal treatments that completely relax the stresses in the formed MG so that the foil retains the shape of the die after its removal ($R = R_0$) [15].

Although Fe-based MGs containing chromium favour a high shaping factor [15], Metglas 2605S3A was selected because the presence of chromium enhances corrosion resistance [25,26], a property that is critical for a wide range of applications, especially in aggressive environments encountered in aerospace and marine engineering.

After TEP, bend tests were performed at room temperature on the shaped (annealed) MG foils. If the foil could be bent flat through 180° without breaking, it was deemed to be still plastic and not embrittled. The mechanical response of the shaped MG foils on normal loading was evaluated by load-displacement measurements carried out using an MTS System compression test machine. A small pre-load was applied to ensure contact between the foil and the crossheads.

The structures of the as-cast and shaped foils were examined using X-ray diffraction (XRD) with monochromatic Cu-Kα radiation using a step size of 0.04° in a Rigaku DMAX diffractometer equipped with a graphite monochromator. Scanning electron microscopy (SEM) images were obtained in a LEO S440 scanning electron microscope (Leica/Cambridge).

3. Results

3.1. Linear wave springs fabricated from metallic-glass foil

The shaping assembly was introduced into a pre-heated furnace at the chosen annealing temperature T_a. Once T_a was reached, the shaping assembly was treated isothermally for 2 min, then quenched in water. The shaping factor increases linearly with T_a (Fig. 1a), and the shaped foils retain their plasticity for values of T_a below ~335°C (denoted here as T_{embrit}). Annealing at higher temperatures leads to higher shaping factors but induces thermal embrittlement of the MG foils, and therefore cannot be considered for practical applications as spring materials. An MG foil after shaping at T_a = 330°C (shown in Fig. 1b) is not embrittled by this TEP.

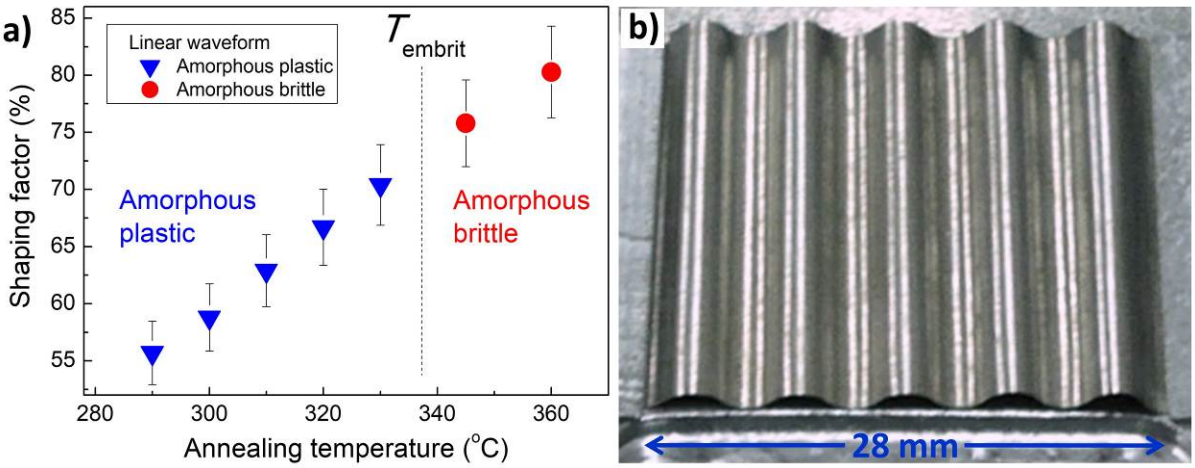

Fig. 1. Fe-based MG foil shaped into a linear wave spring. (a) Shaping factor as a function of the temperature for 2-min anneals, and the thermal embrittlement threshold at T_{embrit}. (b) Top view of the MG foil shaped at 330°C. This linear wave spring has a mass of ~110 mg.

Figure 2 shows how the MG linear wave spring behaves under normal loading. A shaped foil of ~110 mg mass sustains loads up to 140 N (Fig. 2b), remaining entirely in the elastic regime, and indicating promise as a durable and ultra-light flat spring. More interesting is that with further loading, the elastic deformation induces buckling of the waveform, leading to a doubling of the number of the arcs (in this limited length, from five to nine) while sustaining loads up to 270 N (Fig. 2c). After unloading, the waveform with a doubled number of arcs (Fig. 2c) returns to the initial stress-free waveform (Fig. 2a). This reversibility can be achieved only because of the exceptionally high elastic strain limit ($\varepsilon_{el} \approx$ 2%) of MGs, and is assisted by the high ratio of wavelength to foil thickness.

Fig. 2. Side-view snapshots of the shaped MG foil during use as a linear wave spring. (a) Free-standing pre-shaped MG foil. (b) Elastic deformation at the maximum load when still functioning as conventional wave spring. (c) The undulatory behaviour in which further loading leads to elastic multiplication of the number of arcs in the waveform and to an increase in the load capacity.

Figure 3 depicts the load-displacement behaviour during loading and unloading of a pre-shaped MG foil. Up to 140 N, the foil behaves as a non-linear flat spring, the spring stiffness increasing steadily from 120 to 460 N mm^{-1}. The maximum stored elastic energy for this first stage of operation of the wave spring is ~26.6 mJ (i.e. ~1773 kJ m^{-3} per unit volume of material). With further loading, the foil enters a transition zone, in which the formation of each additional arc causes an instant drop in load while at the same time additional elastic energy is stored. When more arcs are formed, the new waveform works as a different flat spring, attaining a load capacity higher than 270 N and a spring constant (~1780 N mm^{-1}) that is more than one order of magnitude higher than in the initial configuration.

In the transition zone, there is clear hysteresis: for a given displacement, the load on loading is always higher than on unloading. This is similar to the undulatory behaviour of a non-pre-shaped MG foil [19,20]. In effect, significant overloading is required to nucleate the new arcs by buckling. The stored energy is that returned on unloading, and is significantly less than the energy expended on loading. For the maximum load shown in Fig. 3, the total elastic energy stored in the MG linear wave spring with the additional ability of its waveform multiplication reaches 39 mJ (i.e. 2600 kJ m^{-3} per unit volume of material).

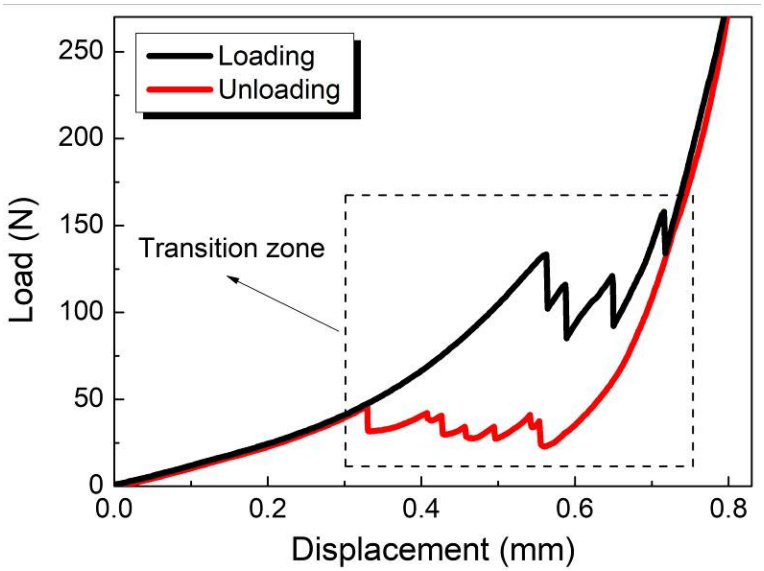

Fig. 3. Load as a function of displacement during loading and unloading of the linear wave spring made by pre-shaping an MG foil. The transition zone is characteristic of MG foils, and corresponds to the undulatory behaviour in which additional arcs are generated (Fig. 2c).

Figure 4 shows the morphology of an MG foil before and after loading to 200 N. Systematic SEM examination did not detect any cracks or shear-bands on the surface of the foils submitted to loading and unloading tests in this study. The response of the wave springs appears to be completely elastic, with no plastic deformation.

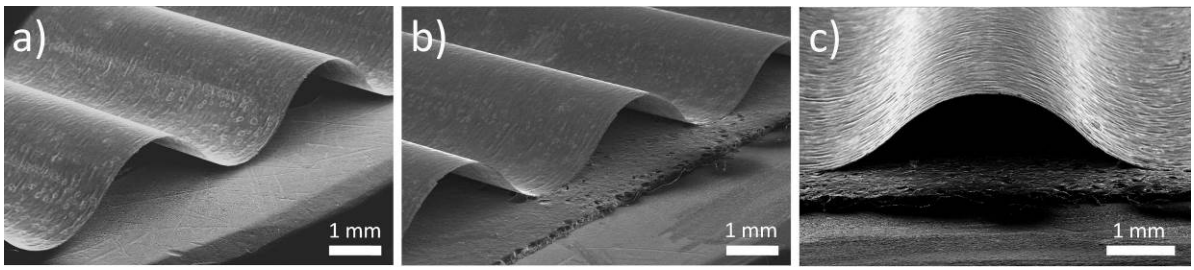

Fig. 4. SEM images of an MG foil patterned into a linear wave spring: (a) after TEP to pre-shape; (b,c) after loading up to 200 N and unloading.

Linear wave springs made of conventional spring materials are commercially available, with working loads from tens to thousands of newtons [23]. This wide range is achieved by changing the spring's characteristics, i.e. number of the arcs, thickness, and length. It is of interest to consider the maximum working load in relation to the volume of the spring material in order to compare the performance of the commercially available wave springs with that of the shaped MG foils in the present study (Fig. 5). Within the range of operation

of the pre-shaped MG foil (i.e. with a fixed number of arcs), the material volume to sustain a given load can be more than one order of magnitude less (blue area, Fig. 5) for the MG foil compared to the conventional linear wave springs. When, under compression, the MG foil multiplies the number of arcs (Fig. 2c), the spring stiffness increases, and the material volume to sustain a given load can be nearly two orders of magnitude less (red area, Fig. 5) for the MG foil.

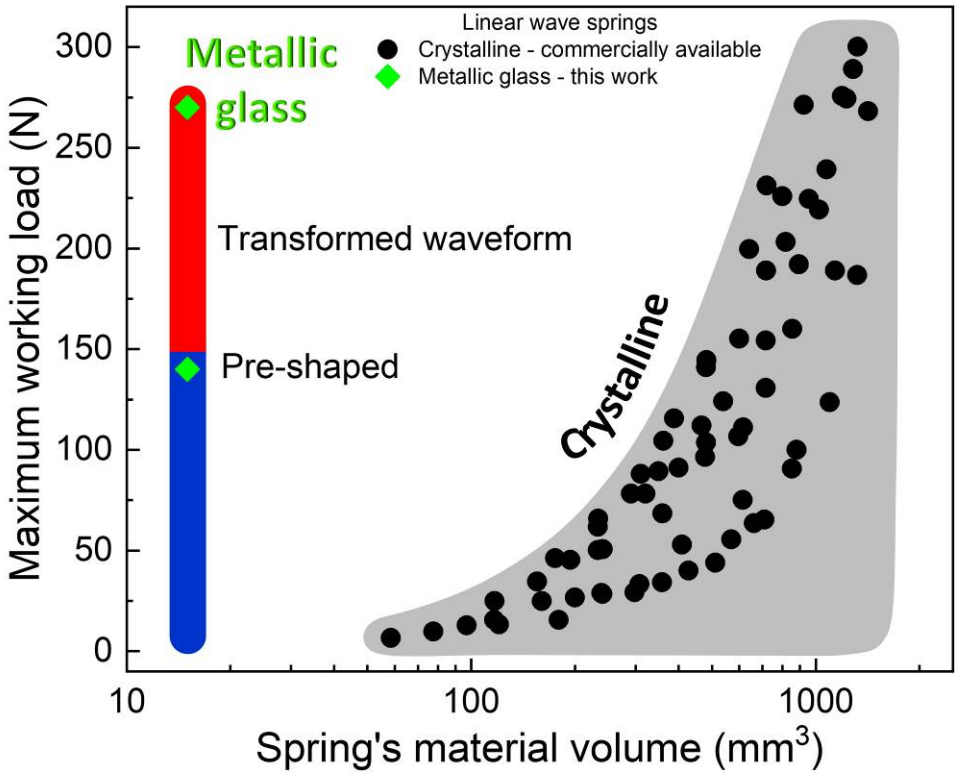

Fig. 5. Performance comparison of commercially available crystalline (black circles) with the MG (green diamonds) linear wave springs. The grey area maps the maximum working load of each individual commercial crystalline spring product [23]. The blue and red areas refer respectively to the working load of the pre-shaped and transformed waveform of the MG linear wave springs.

3.2. Annular wave springs fabricated from metallic-glass foil

The rings cut from the MG foil (Fig. 6a) were subjected to TEP in a stainless-steel die (Fig. 6b,c) to obtain the desired waveform. The TEP was performed by placing the die assembly in a furnace at 450°C. The heating rate experienced by the MG foil is affected by the thermal mass of the die, and the heating profile is shown in Fig. 7a; this is measured by placing a thermocouple in the position of the MG foil in the shaping assembly. Because of

the thermal mass of the annular die, the heating is much slower than in the TEP of the linear waveform.

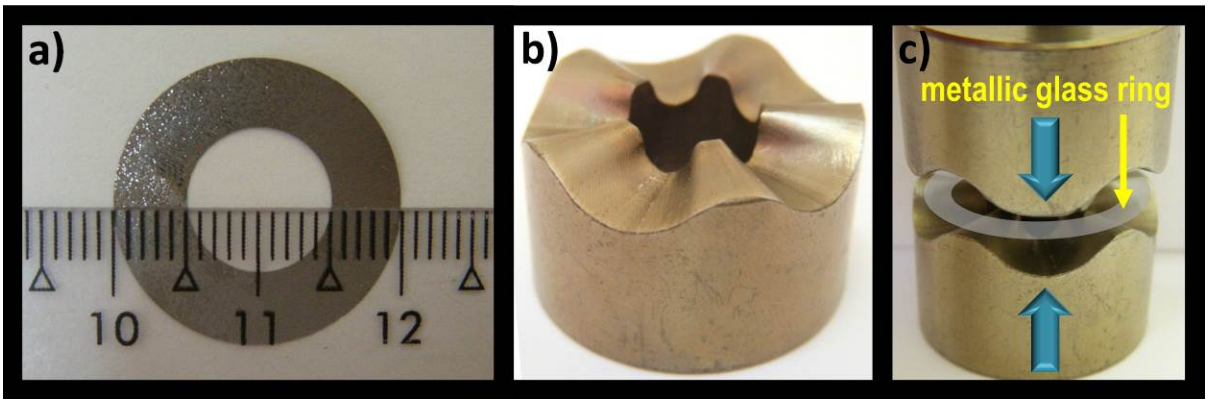

Fig. 6. Unshaped MG ring and the annular waveform die. (a) Ring (mass ≈ 35 mg) cut from an Fe-based MG foil by electroerosion. (b) The bottom part of the stainless-steel die. (c) Both parts of die that impose the waveform on the MG ring.

Samples were processed for different times in the furnace to achieve the desired final annealing temperature T_a, then the shaping assembly was removed and quenched. As for the linear wave spring (Fig. 1a), the shaping factor increases roughly linearly with T_a (Fig. 7b). Values of T_a higher than 295°C lead to thermal embrittlement of the MG foils. Compared to the TEP of the linear wavy patterns discussed previously (Fig. 1a), the threshold temperature T_{embrit} is ~40°C lower. This is a consequence of the lower heating rate, meaning longer annealing times.

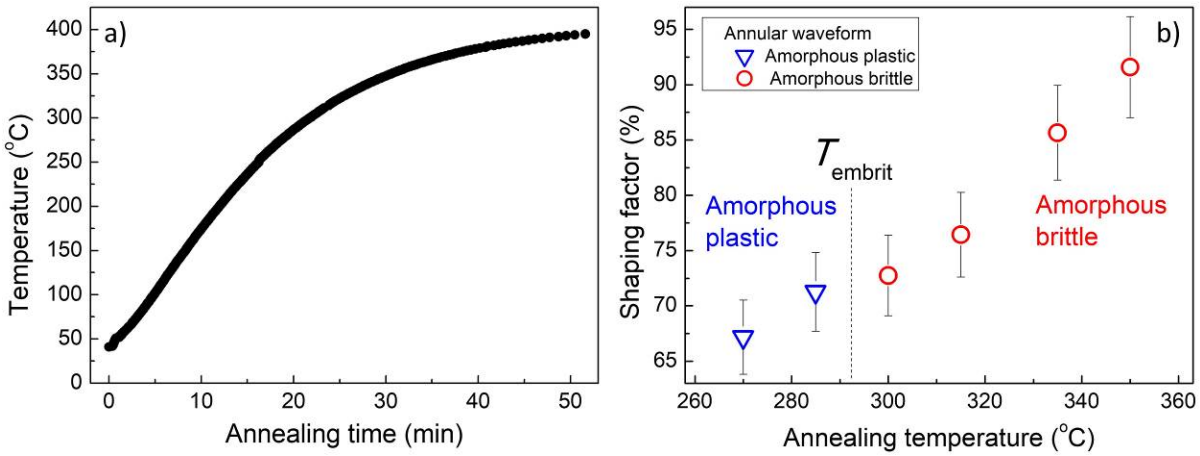

Fig. 7. Fe-based MG foil shaped into an annular wave spring. (a) Heating profile for TEP of a sample in the annular die placed in a furnace at 450°C. (b) Shaping factor as a function of the final anneal temperature, and the thermal embrittlement threshold at T_{embrit}.

Thus, with annealing temperatures below 295°C, the foils can retain the imposed shape with a shaping factor better than 70%, while maintaining their plasticity. As for the linear wave springs, higher T_a would give higher shaping factor, but the embrittlement rules out any practical application.

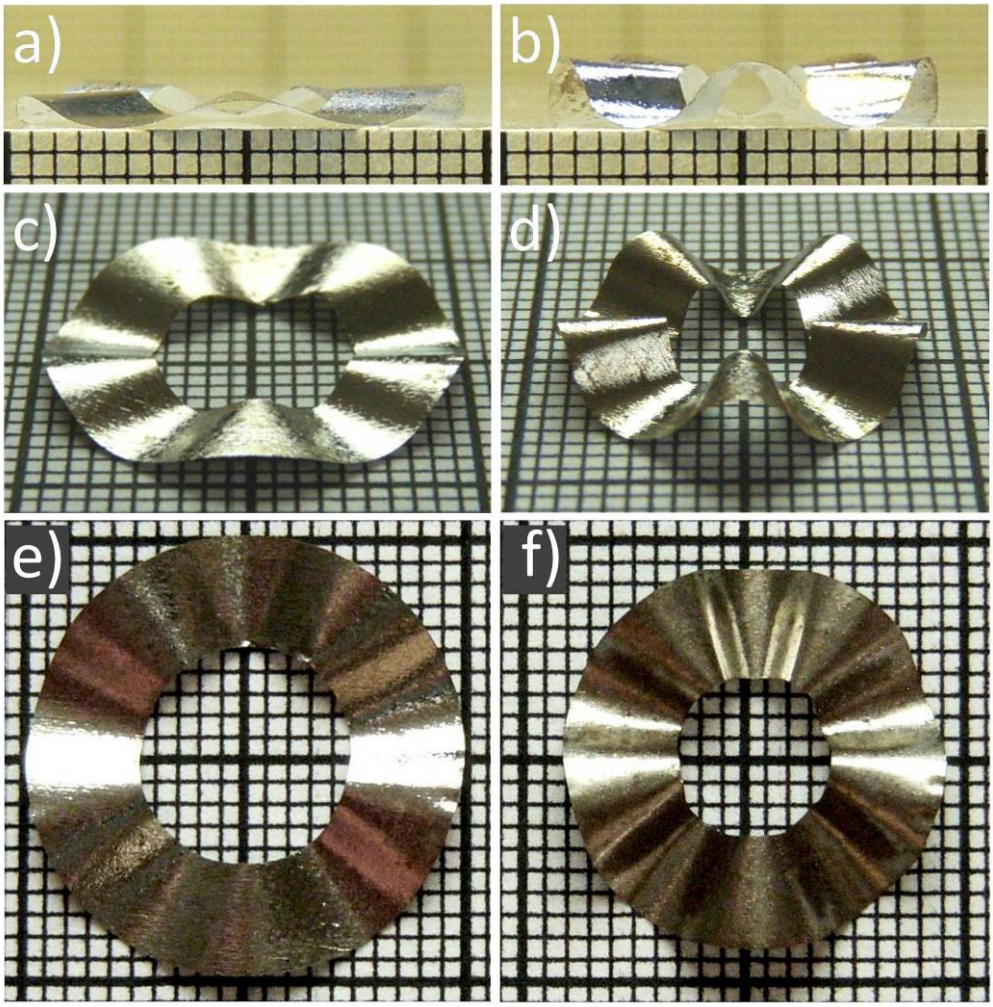

Fig. 8. Annular wave springs formed by TEP of MG foils. (a,b) Side-view of wave springs with the maximum shaping factor achievable for (a) $T_a < T_{embrit}$ (plastic) and (b) $T_a > T_{embrit}$ (brittle). (c,d) The corresponding 45° views. (e,f) The corresponding top views.

Figure 8 compares MG annular wave springs, focusing on the maximum shaping factors that can be achieved below the embrittlement threshold and above it. Given the slower heating and longer times for TEP in the annular die, it was appropriate to check if the shaped foils remain fully amorphous. X-ray diffractograms (Fig. 9) show that this is the case, with no detectable structural change from the as-cast amorphous alloy.

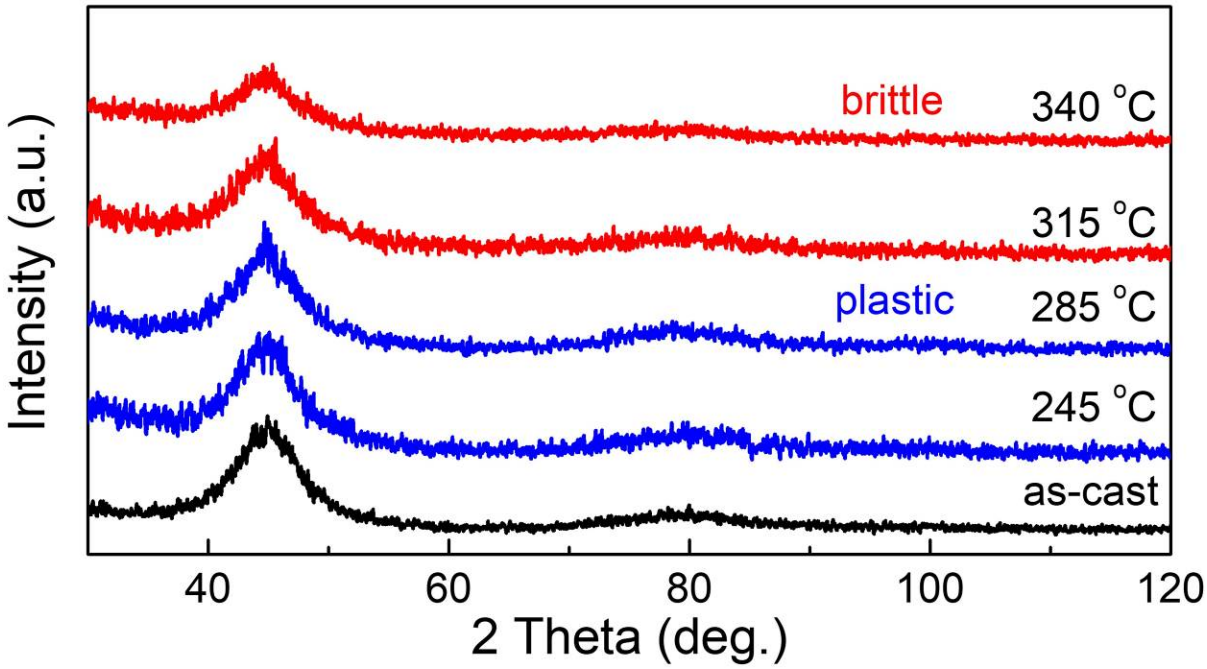

Fig. 9. X-ray diffractograms of Fe-based MG foils. An as-cast foil (black trace) is compared with foils subjected to TEP in the annular die: heated to T_a = 245°C and 285°C, and remaining plastic (blue); heated to T_a = 315°C and 340°C, and embrittled (red).

To exploit the undulatory behaviour of MG foils, an annular waveform was designed to allow doubling of the number of arcs in a similar way to that observed in Section 3.1. The MG foil shaped into an annular waveform was placed on a flat surface with the bottom crests fixed with glue to avoid drifting during loading. When a normal load is applied on the top of the wave spring, new arcs are generated at each original crest, enormously increasing the load capacity of the spring. Figure 10 shows stages during the formation of an additional arc at the crest of one of the five arcs that compose the original annular waveform.

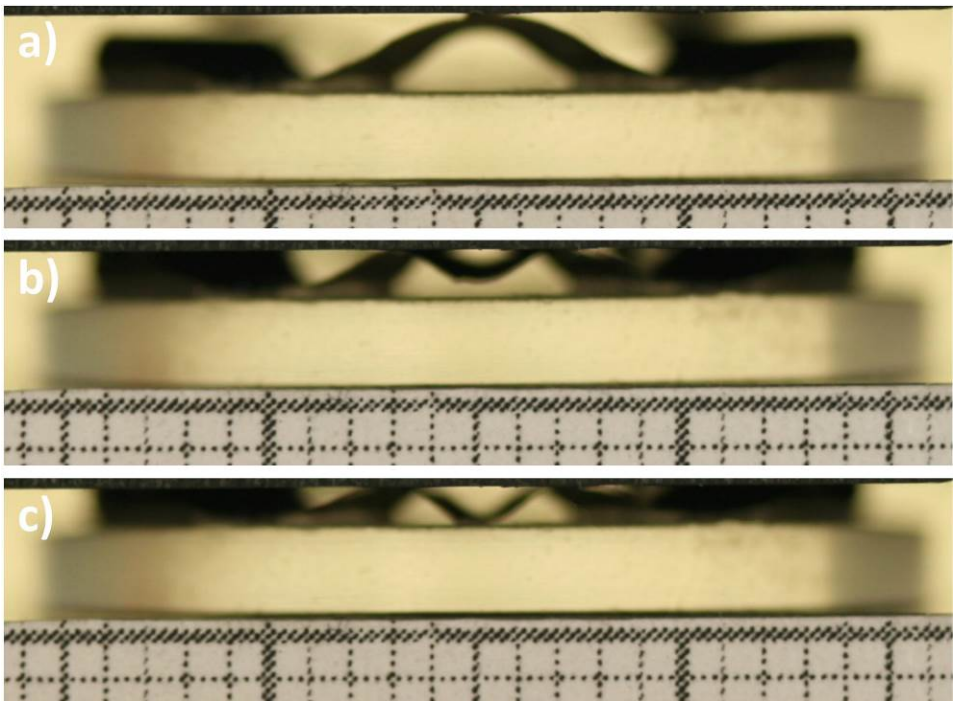

Fig. 10. Side-view snapshots during loading of an Fe-based MG foil shaped into an annular wave spring: (a) at zero load; (b) intermediate stage and (c) final condition of the additional arc formation through the undulatory behaviour that is characteristic of MG foils.

Figure 11 depicts the load-displacement behaviour during loading and unloading of the MG annular wave spring. In this case, the transformation zone spans from ~0.3 mm to ~1.3 mm. With its original waveform, the MG spring can sustain loads of up to ~7 N, storing ~1.2 mJ (i.e. 254 kJ m^{-3} per unit volume of material). The maximum load capacity of 450 N is reached after the formation of the additional arcs. On loading, the detectable generation of new arcs appears to be completed for loads less than 100 N and displacements less than 1.2 mm (though the transition zone, judged from the evident hysteresis, continues to much higher values). The effective spring stiffnesses for loads between 65 N, at the last instant detectable load drop originated by the nucleation of new arcs, and 450 N range from 1500 to 6500 N mm^{-1}. The hysteresis associated with the transition zone extends over a range of load that is much wider than for the linear wave spring (Fig. 3). Much more energy is expended on loading than is returned on unloading. For the maximum load, the total energy stored in (i.e. released on unloading) the MG annular wave spring is ~11.2 mJ (i.e. ~2378 kJ m^{-3} per unit volume of material). This is less than in the MG linear wave springs, but much higher loads can be sustained.

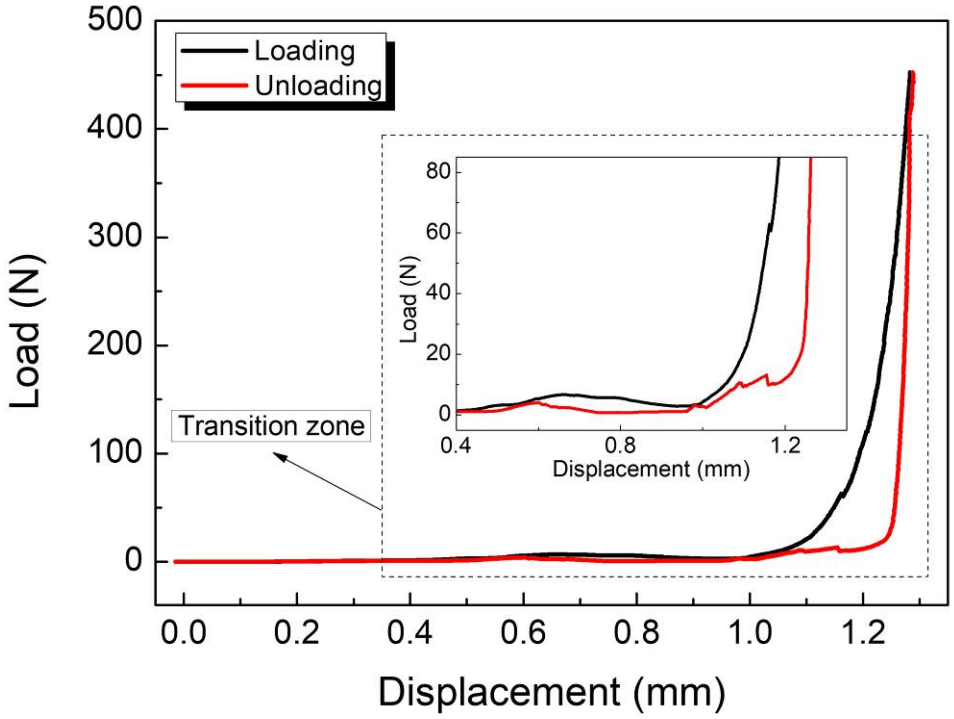

Fig. 11. Load as a function of displacement during loading and unloading of the annular wave spring made by pre-shaping an MG foil. The region within the transition zone, in which the number of arcs in the spring doubles under load, is highlighted in the inset.

Figure 12 shows the maximum working load of, and the volume of material in, commercial wave spring washers [27], and compares with the characteristics of an annular pre-shaped MG foil in the present work. With its original waveform, the MG spring can sustain up to 7 N, a load capacity that is comparable with commercial washers. On further compression, through and above the region of arc multiplication, the load capacity of the MG spring increases, and its material volume, capable of supporting the same load, can be more than two orders of magnitude less than the counterpart commercial washers.

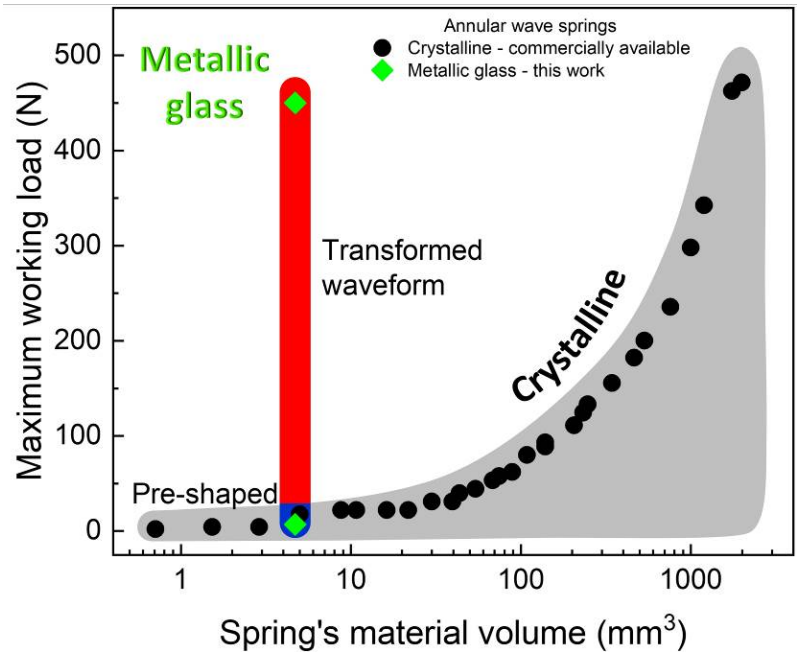

Fig. 12. Performance comparison of commercially available crystalline (black circles) with the MG (green diamonds) annular wave springs (wave spring washers). The grey area maps the maximum working load of each individual commercial crystalline spring product [27]. The blue and red areas refer respectively to the working load of the pre-shaped and transformed waveform of the MG annular wave springs.

Both linear and annular MG wave springs can be produced with various dimensions. The foil's thickness and width, and the amplitude and the number of the formed arcs may be varied to achieve particular load capacities, displacements and stored energies. Figure 13a shows shaped MG annular wave springs with a variety of inner and outer diameters. In addition, assemblies can be designed, such as a simple stacking of the individual waveforms (Fig. 13b,c). A "crest to crest" stacking is used in some conventional crystalline wave spring washers, and such an assembly could also be used to exploit the exceptional mechanical properties of MGs (Fig. 13d–g).

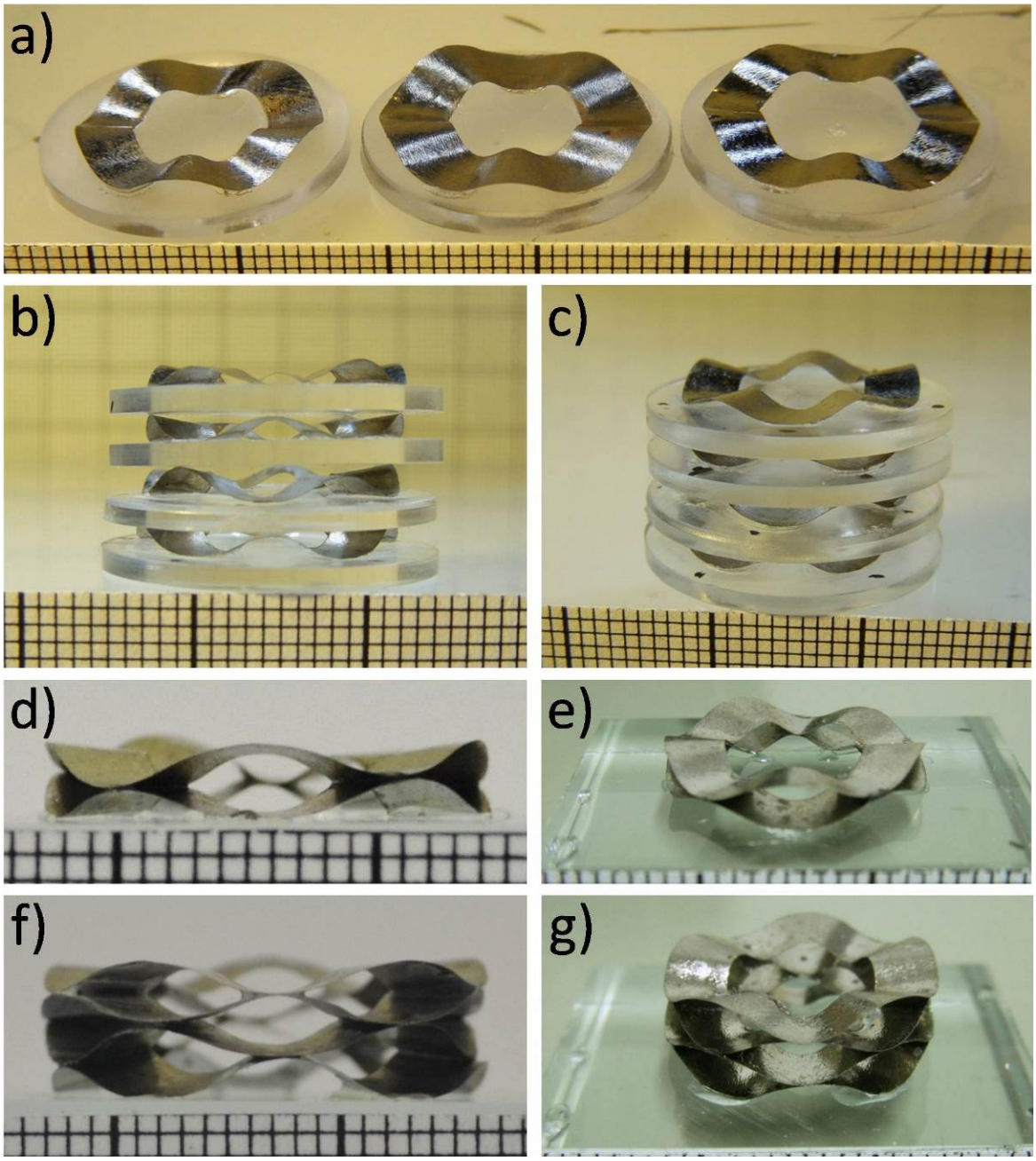

Fig. 13. Assemblies of MG annular wave springs. (a) Single-turn wave springs with a variety of inner and outer diameters. (b,c) Stacking assembly of individual wavy patterns. MG wave spring washers assembled from (d,e) two, and (f,g) four individual waveforms.

4. Discussion

4.1. Applicability of thermo-elastic processing of metallic glasses

The basis of TEP of MGs is that, when annealed under elastic deformation, the sample flows so that the imposed stress is relieved and the desired shape is adopted. But the atomic

mobility that permits stress relief also permits structural relaxation that can lead to embrittlement. Thus, TEP involves a trade-off between the extent of shaping that can be achieved and the extent of embrittlement of the MG. This trade-off has been analysed by Aljerf et al. [15], who show that starting with a less relaxed glass (e.g. a glass obtained on faster quenching) favours shaping without significant embrittlement. This is also favoured in MG compositions that show intrinsically higher resistance to embrittlement [28].

In any case, there is a need to find an optimal time-temperature processing window for the TEP. This window depends upon heating and cooling rates, and thus should be defined for each of the different heating methods and different die geometries used. In the TEP in the present work, the attainable heating rates are one order of magnitude higher for the linear waveforms than for the annular waveforms. The MG in the present work, developed for its soft-magnetic properties, is in a family noted for its tendency to severe embrittlement on annealing [15]. Nevertheless, useful shaping without significant embrittlement has been achieved for both linear and annular waveforms. This indicates that the processing window is wide and not an obstacle to the development of shaped MG foils, for example, for springs.

4.2. Performance and working limit of metallic-glass wave springs

For simple uniaxial loading, the ideal maximum elastic energy that can be stored in a material, per unit volume of the material, can be expressed as $E\varepsilon_{el}^2/2$, where E is Young's modulus. Mapping this ideal storage capacity vs E shows a wide range of behaviour for materials (Fig. 14) [29]. From this range, we focus on the MG in the present study and on conventional spring materials: spring steels and copper-beryllium alloys. For comparison also other TM-based (TM= Zr, Ti, Pd, Co) MGs of high ideal stored elastic energy are displayed [30]. In this limited comparison, the Fe-based MG has the highest value, 40,000 kJ m^{-3}, of maximum ideal stored energy per unit volume.

It is also of interest to consider how much energy would be stored for a given elastic strain in the material; that is simply proportional to E and is highest for conventional spring steels.

It was already known that a flat MG foil elastically shaped into an arc would, under compression, show an undulatory behaviour in which additional arcs are generated [19]. The present work has demonstrated that this undulatory behaviour applies also for linear and annular wave springs made by pre-shaping MG foils. As shown in the load-displacement curves for both types of spring (Figs. 3 and 11) there is a wide transition zone in which

additional arcs appear (on loading) and disappear (on unloading). On either side of the transition zone, the number of arcs in the springs is constant, and there are simpler regimes in which the loading and unloading curves superpose. We consider the energy stored in each of these regimes. For the low-load regime (i.e. with the original number of arcs), the stored energy per unit volume of material is as high as 1773 kJ m^{-3} for the linear spring and 254 kJ m^{-3} for the annular spring, i.e. 4.4% and ~0.6% of the ideal maximum value. And for the ultimate load (after the multiplication of the number of arcs), the stored energy is as high as 2600 kJ m^{-3} for the linear spring and 2380 kJ m^{-3} for the annular spring, i.e. 6.5% and 6% of the ideal maximum value. Noting that a foil bent uniformly to the elastic limit on its surfaces can store only one-third of the elastic energy ideally possible with uniaxial loading, these are high fractions of the ideal value, showing the merit of in the thin-foil geometry used in this work.

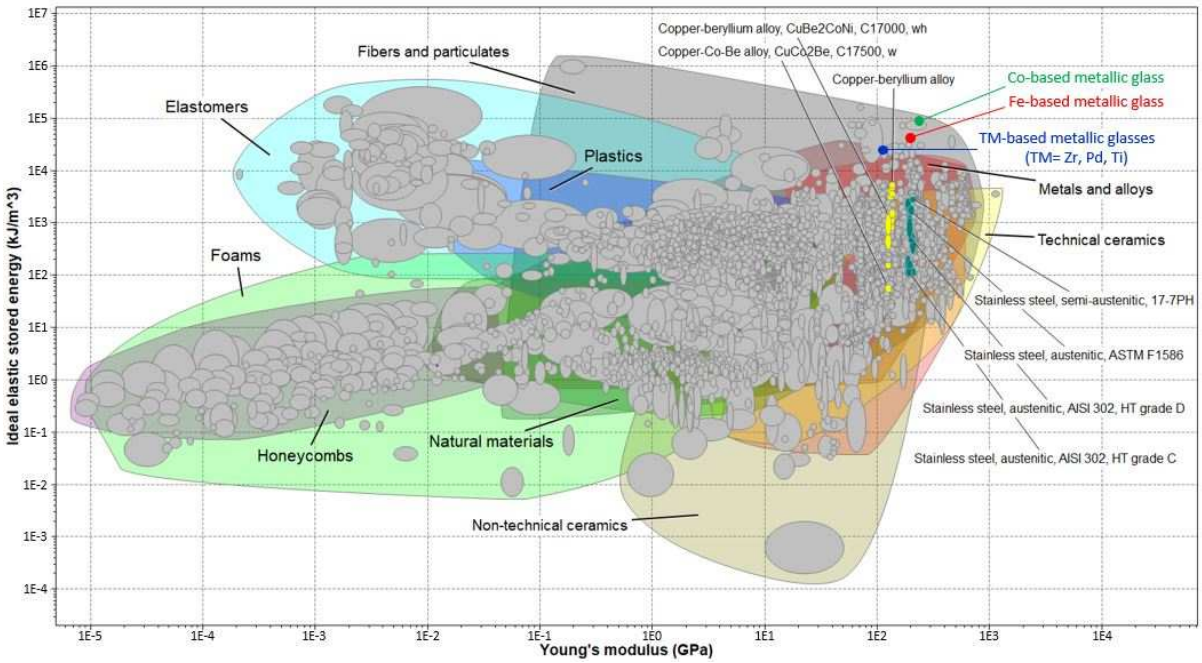

Fig. 14. Mapping of the ideal maximum possible stored elastic energy per unit volume vs Young's modulus for the materials in the *CES EduPack* database [29]. Highlighted are: (TM)-based (TM= Zr, Pd, Ti) MGs (blue dot), Fe-based MG (red dot), Co-based MG (green dot); copper-beryllium alloys (in yellow); and various steels (in cyan).

It is remarkable that the MG wave springs can reversibly support such very high loads: the linear spring can support a load that is ~2.5×10^5 times its own weight, and the annular spring can support ~1.3×10^6 times its own weight. The working regime of these MG wave

springs is, however, unlikely to be at high loads beyond the transition zone. The hysteresis in this zone would lead to large energy dissipation on each loading/unloading cycle, and the stochastic appearance and disappearance of arcs would make the spring behaviour variable. Although in the present work there is no evidence for damage to the MG foils on cycling through the transition zone (Fig. 4), it cannot be excluded that damage may occur over many cycles; the forces on the foils are extreme and effects of fatigue and abrasion are likely. The appropriate limit for normal operation of an MG wave spring would be the maximum load sustainable by the initial waveform. Further investigation is needed to explore the functionality and fatigue life of the MG springs operating through and above the multiplication region.

Nevertheless, it is advantageous to have: (i) the capacity for undulatory behaviour and transition into a regime of much higher spring constant, and (ii) the lack of damage over several cycles through that transition. Figures 3 and 11 show that after one cycle through the transition zone, the elastic performance of the wave springs is retained fully, with the original spring constants recovered. The significance of the undulatory behaviour is, then, that it provides an important fail-safe mechanism in case of overload. Such a resistance to occasional (but potentially very large) overloads would not be found in commercially available crystalline wave springs.

A non-linear spring (i.e. with multiple spring constants) is of interest for shock absorption and vibration isolation [31–35]. The overall trend to much greater stiffness at higher loads (Figs. 3 and 11) is seen also in the "J-shaped" stress-strain curves found for several biomaterials (e.g. ligament) where the non-linearity is considered important for fail-safe mechanical stability [36].

4.3. Application of metallic-glass wave springs in MEMS

In micro-electro-mechanical systems (MEMS), thin metallic parts of various shapes and patterns, including wave, coil and flat springs, are of interest for applications in sensors and actuators [37–45]. There are opportunities in expanding the range of materials that are used [46], and there is particular interest in MGs [47–54]. MGs can be formed by a variety of thin-film deposition methods, and can readily be fabricated in the shapes most commonly found in MEMS devices. TEP has already been used to form a spring from a deposited thin-film MG [53]. MGs exhibit limited plastic strain before fracture (especially in tension) because their deformation is localized in thin shear bands. But for sub-micrometre dimensions, shear-band

nucleation is suppressed, essentially eliminating any problems with lack of MG plasticity [7,55–58].

The present work has shown (Figs. 5 and 12) that in the first stage of loading in which the springs retain the original number of arcs, the MG linear wave spring has a material volume that is up to one order of magnitude smaller than its crystalline counterparts operating at the same load. For the maximum possible loading, after the multiplication of the number of arcs, both linear and annular MG springs have material volumes that are up to two orders of magnitude smaller than their crystalline counterparts. Accordingly, the MG wave springs also have remarkably high values of stored energy per unit volume of material and of supported load and stored energy per unit weight.

Wave springs are conventionally noted for high values of supported load and stored energy per unit volume of the spring. The use of MGs seems capable of significantly increasing these values. The undulatory behaviour that is characteristic of MG foils is associated with the limited foil thickness, and the present results suggest that this behaviour can be beneficial. The thinner foils possible by deposition methods in MEMS device fabrication may offer yet further property enhancements for springs.

5. Conclusions

Thermo-elastic processing over a wide range of conditions can be used to shape metallic-glass foils without thermal embrittlement. Assisted by rapid heating and short annealing times, the shaping is achieved by relief of the elastically imposed stresses while minimizing the degree of structural relaxation of the MG. By TEP, MG foils were shaped into linear and annular wave springs. Stacked assemblies of annular springs have also been made. Under compression, the springs show a distinctive undulatory behaviour in which the number of arcs in the waveform increases. This increases the maximum load capacity and the spring constant. Both the linear and annular wave springs formed by shaping MG foils can sustain a wide range of loads similar to those for commercially available linear wave springs and wave spring washers. But the MG springs have a material volume that is one to two orders of magnitude smaller than for the springs (of the same load-bearing capacity) made from conventional crystalline materials. An MG linear wave spring of mass 110 mg can support a load conventionally (with a fixed number of arcs in the spring) of 140 N, and after the arcs have multiplied as a result of the undulatory behaviour, can support an ultimate load of 270 N. An MG annular wave spring of mass 35 mg can support a load conventionally of 7

N, and after arc-multiplication can support an ultimate load of 450 N. The linear and annular springs can, without damage, support loads that are, respectively ~2.5×10^5 times and ~1.3×10^6 times their own weight. MGs, in general, are known to be attractive as spring materials, and the particular Fe-based MG in the present study has an ideal elastic-energy storage capacity of 40,000 kJ m^{-3}, far exceeding that of common, crystalline spring materials. Per unit volume of material, the wave springs can store as much as 2600 kJ m^{-3} (6.5% of the ideal value). The normal working limit of the MG wave springs is likely to be in the conventional regime (fixed number of arcs), but the undulatory behaviour is important in rendering the springs fail-safe even under extreme overload. Conventional wave springs are excellent for action in a restricted volume. The present work shows that this attribute could be improved very significantly through the use of shaped MG foils. In particular, there is great potential for novel wave springs with enhanced mechanical performance, and with reduced volume and weight, in the development of MEMS devices.

Acknowledgements

This work is dedicated to the memory of the late Prof. A.R. Yavari. He initiated this work, and his co-authors gratefully acknowledge his leadership, mentoring and friendship. This work was funded by the ANR Emergence project New Vitrified Springs (Grant # ANR-12-EMMA-0054), the Brazilian funding agency FAPESP (Grant # FAPESP TEMATIC PROJECT- 2013/05987-8), the EU Marie-Curie ITN project VitriMetTech (Grant # 607080 FP7-PEOPLE-2013-ITN), and the EU Horizon 2020 research and innovation programme ExtendGlass (# ERC-2015-AdG-695487). The authors acknowledge, at Université Grenoble Alpes, C. Josserond for providing access and technical support for the load-displacement measurements, and J. Cassan for experimental assistance.

Data availability

The data required to produce these findings are available from the corresponding author upon reasonable request.

References

[1] M.F. Ashby, A.L. Greer, Metallic glasses as structural materials, Scripta Mater. 54 (2006) 321–326.

[2] M. Telford, The case for bulk metallic glass, Mater. Today 7 (2004) 36–43.

[3] A.I. Salimon, M.F. Ashby, Y. Bréchet, A.L. Greer, Bulk metallic glasses: what are they good for? Mater. Sci. Eng. A 375–377 (2004) 385–388.

[4] W.L. Johnson, Bulk amorphous metal- An emerging engineering material, JOM 54 (2002) 40–43.

[5] J. Schroers, Processing of bulk metallic glass, Adv. Mater. 22 (2010) 1566–1597.

[6] A. Inoue, B. Shen, H. Koshiba, H. Kato, A.R. Yavari, Cobalt-based bulk glassy alloy with ultrahigh strength and soft magnetic properties, Nat. Mater. 2 (2003) 661–663.

[7] A.R. Yavari, K. Georgarakis, W.J. Botta, A. Inoue, G. Vaughan, Homogenization of plastic deformation in metallic glass foils less than one micrometer thick, Phys. Rev. B 82 (2010) 172202.

[8] S. Roth, M. Stoica, J. Degmova, U. Gaitzsch, J. Eckert, L. Schultz, Fe-based bulk amorphous soft magnetic materials, J. Magn. Magn. Mater. 304 (2006) 192–196.

[9] P. Tiberto, M. Baricco, E. Olivetti, R. Piccin, Magnetic properties of bulk metallic glasses, Adv. Eng. Mater. 9 (2007) 468–474.

[10] J.R. Scully, A. Gebert, J.H. Payera, Corrosion and related mechanical properties of bulk metallic glasses, J. Mater. Research 22 (2007) 302–313.

[11] N. Li, W. Chen, L. Liu, Thermoplastic micro-forming of bulk metallic glasses: A review, JOM 68 (2016) 1246–1261.

[12] W.J. Botta, A.M. Jorge, M.J.E. Rodrigues, C.S. Kiminami, C. Bolfarini, M.F. de Oliveira, A.R. Yavari, Electromechanical processing of bulk metallic glasses, J. Metastable Nanocryst. Mater. 15–16 (2003) 11–16.

[13] G. Kaltenboeck, M.D. Demetriou, S. Roberts & W.L. Johnson, Shaping metallic glasses by electromagnetic pulsing, Nat. Comm. 7 (2015) 10576.

[14] P. Yiu, C.H. Hsueh, C.H. Shek, Rapid thermoplastic formation of Fe-based metallic glass foil achieved by electropulsing, Mater. Lett. 136 (2014) 353–355.

[15] M. Aljerf, K. Georgarakis, A.R. Yavari, Shaping of metallic glasses by stress-annealing without thermal embrittlement, Acta Mater. 59 (2011) 3817–3824.

[16] K. Russew, L. Stojanova, Glassy Metals, Springer-Verlag Berlin, 2016.

[17] K. Son, H. Soejima, N. Nishiyama, X.-M. Wang, A. Inoue, Process development of metallic glass wires by a groove quenching technique for production of coil springs, Mater. Sci. Eng. A 449–451 (2007) 248–252.

[18] A. Inoue, N. Nishiyama, New bulk metallic glasses for applications as magnetic-sensing, chemical, and structural materials, MRS Bull. 32 (2007) 651658.

[19] N.T. Panagiotopoulos, M.A. Yousfi, K. Georgarakis, A.R. Yavari, Mechanically induced waves in metallic glass foils, Mater. Des. 90 (2016) 1110–1114.

[20] M.A. Yousfi, N.T. Panagiotopoulos, A.M. Jorge Junior, K. Georgarakis, A.R. Yavari, Novel micro-flat springs using the superior elastic properties of metallic glass foils, Scripta Mater. 131 (2017) 84–88.

[21] W.H. Jiang, F.X. Liu, Y.D. Wang, H.F. Zhang, H. Choo, P.K. Liaw, Comparison of mechanical behavior between bulk and ribbon Cu-based metallic glasses, Mater. Sci. Eng. A 430 (2006) 350–354.

[22] J.F. Löffler, A.A. Kündig, F.H. Dalla Torre, Rapid Solidification and Bulk Metallic Glasses – Processing and Properties, in: J.R. Groza, J.F. Shackelford, E.J. Lavernia, M.T. Powers (Eds.), Materials Processing Handbook, CRC Press, Boca Raton, 2007, page 17-8.

[23] Smalley, Smalley Linear Springs datasheet, Nov. 2019. https://www.smalley.com/sites/default/files/pdfs/LS-2013.pdf

[24] C.A. Schneider, W.S. Rasband, K.W. Eliceiri, NIH Image to ImageJ: 25 years of image analysis, Nat. Methods 9 (2012) 671–675.

[25] C. Suryanarayana & A. Inoue, Iron-based bulk metallic glasses, Int. Mater. Rev. 58 (2013) 131–166.

[26] Z.L. Long, Y. Shao, X.H. Deng, Z.C. Zhang, Y. Jiang, P. Zhang, B.L. Shen, A. Inoue, Cr effects on magnetic and corrosion properties of Fe-Co-Si-B-Nb-Cr bulk glassy alloys with high glass-forming ability, Intermetallics 15 (2007) 1453–1458.

[27] Associated Spring Raymond, "SPEC® Spring Washers", Wave Spring Washers datasheets, Nov. 2019. https://www.assocspring.co.uk/wave-spring-washers.html

[28] J.J. Lewandowski, W.H. Wang and A.L. Greer, Intrinsic plasticity or brittleness of metallic glasses, Philos. Mag. Lett. 85 (2005) 77–87.

[29] CES EduPack software, Granta Design Limited 2019, Cambridge, United Kingdom.

[30] W.H. Wang, The elastic properties, elastic models and elastic perspectives of metallic glasses, Prog. Mater. Sci. 57 (2012) 487–656.

[31] T.-H. Wu, C.-C. Lan, A wide-range variable stiffness mechanism for semi-active vibration systems, J. Sound Vib. 363 (2016) 18–32.

[32] C.-C. Lan, S.-A. Yang, Y.-S. Wu, Design and experiment of a compact quasi-zero-stiffness isolator capable of a wide range of loads, J. Sound Vib. 333 (2014) 4843–4858.

[33] B.A. Fulcher, D.W. Shahan, M.R. Haberman, C. C. Seepersad, P.S. Wilson, Analytical and experimental investigation of buckled beams as negative stiffness elements for passive vibration and shock isolation systems, J. Vib. Acoust. 136 (2014) 031009.

[34] M. Leblouba, S. Altoubat, M.E. Rahman, B.P. Selvaraj, Elliptical leaf spring shock and vibration mounts with enhanced damping and energy dissipation capabilities using lead spring, Shock Vib. 2015 (2015) 482063.

[35] R.A. Ibrahim, Recent advances in nonlinear passive vibration isolators, J. Sound Vib. 314 (2008) 371–452.

[36] S. Vogel, Comparative Biomechanics, Princeton UP, Princeton and Oxford, 2003, page 326.

[37] X. Zhanwen, Z. Ping, N. Weironga, D. Liqun, C. Yun, A novel MEMS omnidirectional inertial switch with flexible electrodes, Sensors Actuat. A 212 (2014) 93–101.

[38] D. Grech, K.S. Kiang, J. Zekonyte, M. Stolz, R.J.K. Wood, H.M.H. Chong, Highly linear and large spring deflection characteristics of a Quasi-Concertina MEMS device, Microelectron. Eng. 119 (2014) 75–78.

[39] Y. Wang, Q. Feng, Y. Wang, W. Chen, Z. Wang, G. Ding, X. Zhao, The design, simulation and fabrication of a novel horizontal sensitive inertial micro-switch with low g value based on MEMS micromachining technology, J. Micromech. Microeng. 23 (2013) 105013.

[40] N. Lu, S. Yang, Mechanics for stretchable sensors, Curr. Opin. Solid State Mater. Sci. 19 (2015) 149–159.

[41] S. Wang, J. Song, D.H. Kim, Y. Huang, J. A. Rogers, Local versus global buckling of thin films on elastomeric substrates, Appl. Phys. Lett. 93 (2008) 023126.

[42] Z. Li, Y. Wang, J. Xiao, Mechanics of curvilinear electronics and optoelectronics, Curr. Opin. Solid State Mater. Sci. 19 (2015) 171–189.

[43] Y. Zhang, Y. Huang, J.A. Rogers, Mechanics of stretchable batteries and supercapacitors, Curr. Opin. Solid State Mater. Sci. 19 (2015) 190–199.

[44] T. Ma, H. Liang, G. Chen, B. Poon, H. Jiang, H. Yu, Micro-strain sensing using wrinkled stiff thin films on soft substrates as tunable optical grating, Opt. Express 21 (2013) 11994–12001.

[45] W.M. Choi, J. Song, D.Y. Khang, H. Jiang, Y.Y. Huang, J.A. Rogers, Biaxially stretchable "wavy" silicon nanomembranes, Nano Lett. 7 (2007) 1655–1663.

[46] S.M. Spearing, Materials issues in microelectromechanical systems (MEMS), Acta Mater. 48 (2000) 179–196.

[47] A. Chauhan, R. Vaish, An assessment of bulk metallic glasses for microelectromechanical system devices, Int. J. Appl. Glass Sci. 4 (2013) 231–241.

[48] N. Nishiyama, K. Amiya, A. Inoue, Bulk metallic glasses for industrial products, Mater. Trans. 45 (2004) 1245–1250.

[49] A.L. Greer, Metallic glasses... on the threshold, Mater. Today 12 (2009) 14–22.

[50] G. Kumar, A. Desai, J. Schroers, Bulk metallic glass: The smaller the better, Adv. Mater. 23 (2011) 461–476.

[51] J.P. Singer, C.I. Pelligra, N. Kornblum, Y. Choo, M. Gopinadhan, P. Bordeenithikasem, J. Ketkaew, S.F. Liew, H. Cao, J. Schroers, C.O. Osuji, Multiscale patterning of a metallic glass using sacrificial imprint lithography, Microsyst. Nanoeng. 1 (2015) 15040.

[52] J. Schroers, Q. Pham, A. Desai, Thermoplastic forming of bulk metallic glass – A technology for MEMS and microstructure fabrication, J. Microelectromech. Syst. 16 (2007) 240–247.

[53] T. Fukushige, S. Hata, A. Shimokohbe, A MEMS conical spring actuator array, J. Microelectromech. Syst. 14 (2005) 243–253.

[54] R. Martinez-Duarte, SU-8 Photolithography as a toolbox for carbon MEMS, Micromachines 5 (2014) 766–782.

[55] D. Jang, J.R. Greer, Transition from a strong-yet-brittle to a stronger-and-ductile state by size reduction of metallic glasses, Nat. Mater. 9 (2010) 215–219.

[56] J.R. Greer, J.Th.M. De Hosson, Plasticity in small-sized metallic systems: Intrinsic versus extrinsic size effect, Prog. Mater. Sci. 56 (2011) 654–724.

[57] L. Tian, Z.-W. Shan, E. Ma, Ductile necking behavior of nanoscale metallic glasses under uniaxial tension at room temperature, Acta Mater. 61 (2013) 4823–4830.

[58] M. Ghidelli, H. Idrissi, S. Gravier, J.-J. Blandin, J.-P. Raskin, D. Schryvers, T. Pardoen, Homogeneous flow and size dependent mechanical behavior in highly ductile $Zr_{65}Ni_{35}$ metallic glass films, Acta Mater. 131 (2017) 246–259.

Thermo-elastically shaped metallic glass wavy patterns

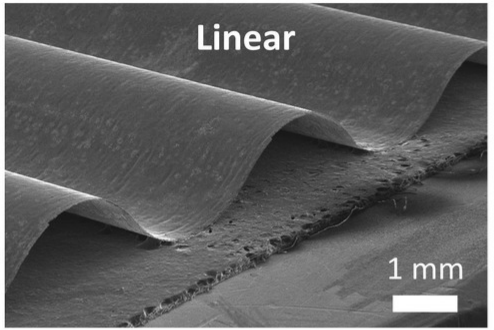

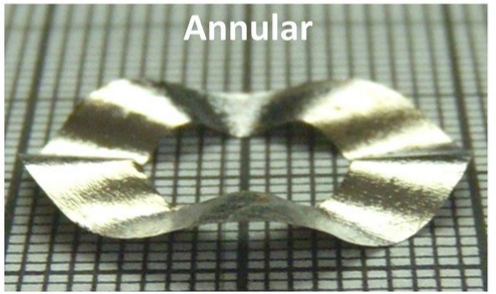

Two-stage reversible undulatory spring behaviour

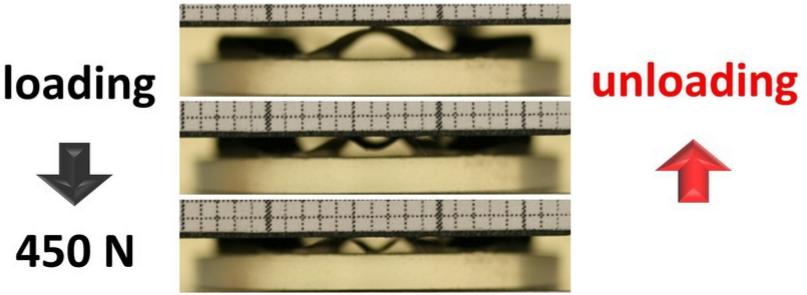

Metallic glass springs performance